# Magnetic turbulence in the core plasma of the CASTOR tokamak

**I. Ďuran[1], K. Jakubka[2], J. Stöckel[2]**
[1]*Faculty of Mathematics and Physics, Charles University, Prague, Czech Republic*
[2]*Institute of Plasma Physics, CAS, Prague, Czech Republic*

**Abstract**
*Link between the transport processes and magnetic turbulence in tokamaks is not clearly understood yet. One of the reasons is that the relevant magnetic data directly measured in the central region of plasma column are not available. The fluctuations of radial magnetic field are monitored by means of array of eight radial magnetic coils well in the plasma interior of the CASTOR tokamak. The measured signal is found to be a superposition of broadband microturbulence and coherent modes (esp. with the poloidal mode number m=2). Standard numerical data processing is applied to characterize these two components individually.*

## 1. Experimental arrangement and calibration.

Some aspects of the magnetic turbulence are investigated on the CASTOR tokamak ($R = 0.4\ m,\ a = 0.085\ m,\ B_t = 0.5 \div 1.1\ T,\ I_p = 5 \div 20\ kA,\ \tau_d = 50\ ms$). The radial component of the magnetic field $B_r$ is measured by the array of eight absolutely calibrated coils (the diameter of each is 4.4 mm, the length is 4 mm), spaced in the radial direction by 6.7 mm. The total active length of the array is 51 mm, which represents $\sim 60\%$ of the plasma minor radius. Whole array is encased in the stainless steel jacket to provide necessary electrostatic shielding and to protect the coils from the heat overload. In short discharges (t $\leq$ 10 ms) with a reduced plasma current ($I_p \leq 7$ kA), the whole array can be inserted into the plasma column without any damage and plasma is not perturbed significantly. The poloidal component of the magnetic fluctuations $B_\theta$ is measured by the set of 16 Mirnov coils located in the limiter shadow. The position of the magnetic diagnostics in the poloidal cross-section is shown in the Fig. 1.

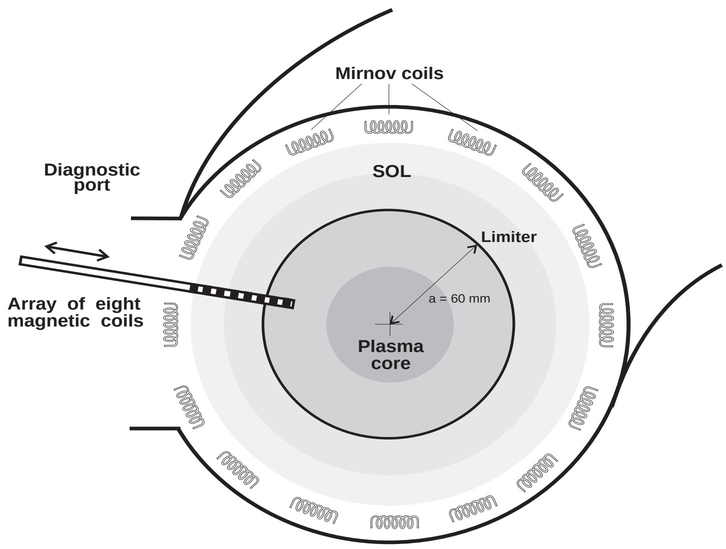


Figure 1: *Position of the magnetic probes in the poloidal cross-section of the CASTOR tokamak.*

A schematic view of the data acquisition system is shown in the Fig. 2. The signals from coils are conditioned by a passive RC integrating circuit to remove high frequency component (> 300kHz) to avoid aliasing. Then, the coil signal is digitized by the 12 bit A/D converter. and data are transferred via an optical insulator to the PC-oriented database. The fastest used sampling rate was 0.2 $\mu s$. The data were recorded within a time interval 2 - 13 ms, depending on the sampling rate.

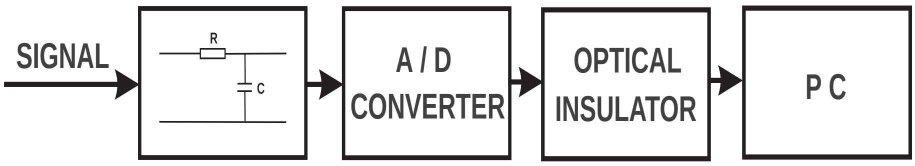


Figure 2: *Block diagram of data acquisition from the magnetic probes.*

Once the data are stored at the PC hard disk, the three step numerical processing is applied, using IDL software package:

- conversion of the raw data into absolute unites,
- their numerical integration
- statistical analysis of these data to characterize the magnetic fluctuations.

All radial magnetic coils are absolutely calibrated. The output voltage of the coil is:

$$V = A_{eff}\frac{dB_r}{dt} \qquad\qquad [Volts, m^2, T/s], \tag{1}$$

where $A_{eff}$ is effective area of the coil (calibration constant) and $dB_r/dt$ is the time derivative of the measured magnetic field. The response of the coil is frequency independent (within 5%) for frequencies (5-300 kHz). It suggests that the electrostatic shielding doesn't reduce the sensitivity of the probe array significantly.

## 2. Experimental results

The fluctuations of radial magnetic field were monitored in discharges with the plasma current in the range $I_p = 6 \div 10\ kA$ and the toroidal magnetic field $B_T = 0.5 \div 1\ T$. The numerical processing of the probes data consisted of the standard spectral and correlation analysis. The interpretation of the lowpass component (< 10 kHz) of the signals is not straightforward therefore, this spectral band is numerically cut off. Generally, the two types of frequency spectra are observed depending on discharge conditions as shown in the Fig. 2. Each window displays the eight frequency spectra of the $B_r$-fluctuations measured by the eight coils array.

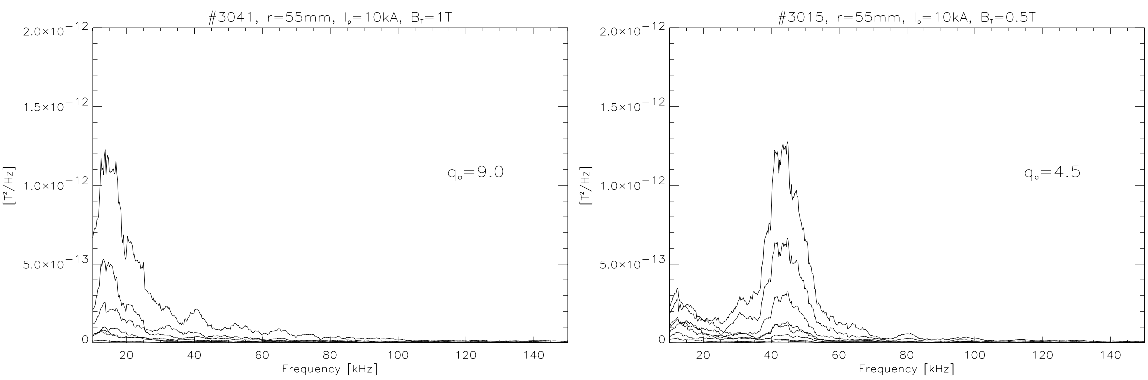


Figure 3: *Power spectral densities computed for two shots with the plasma current $I_p$=10 kA.*
**Left window** : *$B_T$=1 T $\longrightarrow$ safety factor q(a)=9.0*
**Right window** : *$B_T$=0.5 T $\longrightarrow$ safety factor q(a)=4.5*

The left window shows monotonously decreasing spectra with no dominant frequencies. On the other hand, the relatively narrow spectral peak ($\Delta f\ \sim$ 10 kHz) superimposed over the broadband background is clearly identified around dominant frequency 45 kHz in the right window for all the 8 signals. In general, presence of some dominant frequency in the power spectra is characteristic for shots with low safety factor q(a)<8, when the MHD unstable magnetic surfaces with q=1, 2 or 3 can appear within the plasma column. The peaks are not observed for shots with q(a)>8.

Another important spectral characteristic of turbulence is the associated coherence. The coherence has a meaning of frequency resolved correlation and therefore it may give an important insight into the nature of the modes and instabilities. The next figure shows frequency resolved radial profiles of coherence coefficient with reference probe No. 1 for shots with q(a)=9 and q(a)=5.4.

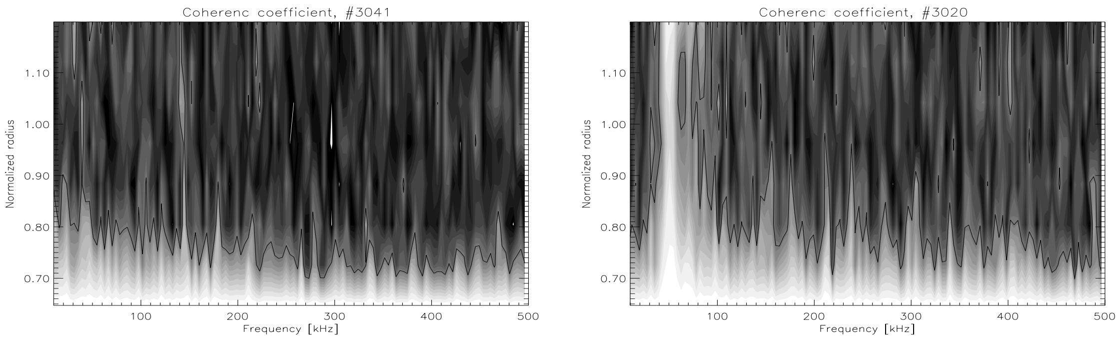


Figure 4: *Coherence coefficient with reference probe No. 1 for:*
**Left window** *: shot #3041 with $B_T$=1 T, $I_p$=10 kA $\longrightarrow$ safety factor q(a)=9.0*
**Right window** *: shot #3020 with $B_T$=0.6 T, $I_p$=10 kA $\longrightarrow$ safety factor q(a)=5.4*

It is seen that coherence for #3041 depicted in the left window, although substantially high, falls rapidly down for probe No. 3 and probes more radially separated from the reference probe No. 1 for all frequencies. It indicates that no global coherent modes are present in plasma under these discharge conditions. On the other hand, for #3020 (right window) coherent radial strip for frequencies around 50 kHz is observed. At these frequencies the coherence coefficient is close to maximum value 1 for all the eight probes. It suggests that some global coherent mode exists in plasma when q(a)<8. It should be also noted that the character of the coherence for frequencies below and above the coherent strip is quite similar.

The Mirnov coils measurements revealed that the dominant frequency in the $B_r$ spectra is associated with the presence of the m=2 magnetic island within the plasma column. This is concluded from the next figure.

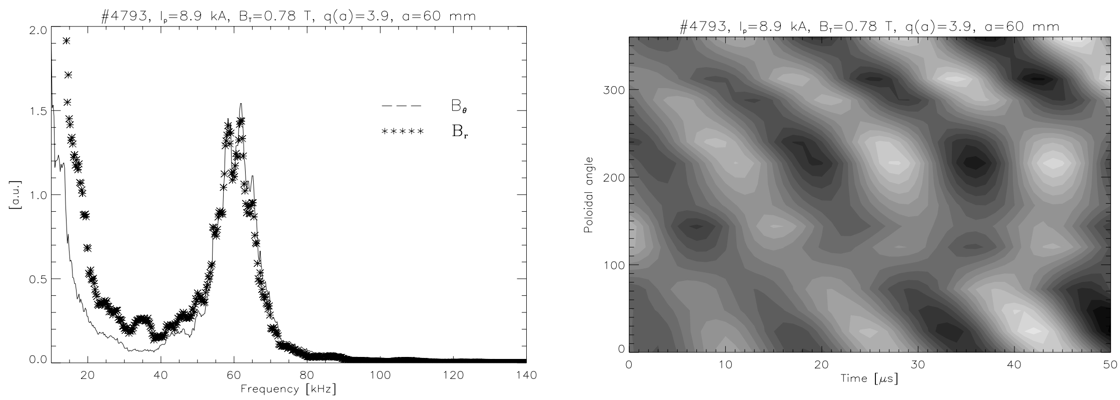


Figure 5: **Left window :** *Frequency spectra of the signal from the Mirnov coil No.2 (solid line) and one radial magnetic coil at r=64 mm (stars) are normalized to fit each other at f=60 kHz (#4793 with $I_p$=8.9 kA, $B_T$=0.78 T, q(a)=3.9 and a=60 mm).*
**Right window :** *Signals from 16 Mirnov coils (angle 0° corresponds to lowfield side midplane, 90° to top, 180° to highfield side midplane and 270° to bottom.*

The left window compares the frequency spectrum of the $\tilde{B}_\theta$ fluctuations measured by one of the Mirnov coils with the spectrum of the $\tilde{B}_r$ fluctuations measured by one of the radial magnetic coils. Both the signals are monitored in the same shot. It is well seen that the $\tilde{B}_\theta$ and $\tilde{B}_r$

spectra are nearly identical in the frequency range f=50÷70 kHz, even including some details. This indicates that both the magnetic probes observe the same phenomenon.

The poloidal mode number of the $\tilde{B}_\theta$ perturbation is determined from the signals of all the Mirnov coils currently in operation[1] displayed in the right window in the $\theta$-t plane. Only a short period (50 $\mu s$ long time interval) is analyzed to resolve well the poloidal distribution and propagation of $\tilde{B}_\theta$ structures. The amplitude of the $\tilde{B}_\theta$ fluctuations is distinguished by shadowing. The bright regions correspond to the maximum of $\tilde{B}_\theta$ while the dark regions are the minima. It is seen that the dark and bright strips exhibit a slope in the $\theta$-t plane, which manifests the poloidal propagation of $\tilde{B}_\theta$ perturbations with angular velocity $\omega \doteq 2 \cdot 10^5\ rad/s$. The sense of this poloidal rotation agrees with direction of the electron diamagnetic drift. Furthermore, it is evident that for every fixed time there are always present two maxima and two minima in the $\theta$-t plane. This directly leads to conclusion that a mode with poloidal number m=2 is present within the plasma column. Such a mode can efficiently grow only around the magnetic surface with q(r)=2. Consequently, the spectral peak in $B_r$ spectra is caused by poloidal rotation of this magnetic island.

Let's emphasize two quantitative aspects of our experimental results:

- The spectral peak observed with magnetic probes is caused by rotation of the coherent mode in the poloidal direction. Its frequency agrees well with the angular frequency deduced from the poloidally resolved measurements with the Mirnov coil:

$$\omega = \frac{2\pi f_{FFT}}{m}$$

  if we take $m = 2$.

- We take the current density profile in a general form:

$$j(r) = j(0)(1 - \frac{r^2}{a^2})^p \quad . \tag{2}$$

  The corresponding radial profile of the safety factor q(r):

$$q(r) = q(a)\frac{r^2/a^2}{1 - (1 - r^2/a^2)^{p+1}} \tag{3}$$

  is displayed in the next figure for two reasonable values of the peaking factor[2] p=1.5, 3.

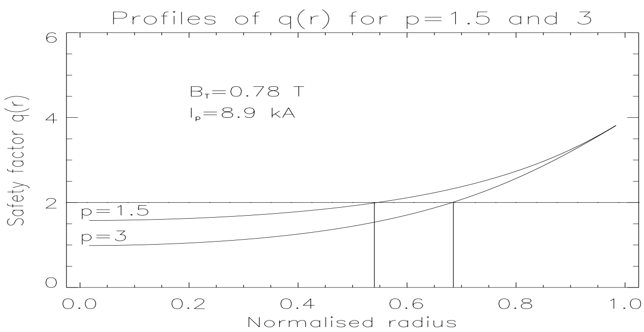


Figure 6: *Radial profile of safety factor q(r) for two values of peaking factor p=1.5 and 3 for shot #4793. The minor radius of the plasma column is a=0.06 m,* $q(a) = 3.9$.

[1] Unfortunately, coils No.1,5,9,12 and 15 were out of operation during these measurements.

[2] A more flat current profiles can be hardly expected, since the electron temperature profile is at least parabolic and $j \sim T_e^{3/2}$. On the other hand, a more peaked profile with $p > 3$ leads to appearance of q=1 surface. Consequently, the m=1 mode would be observed which is not the case of the experiment.

It is seen, that the radial position of the resonant magnetic surface with $q = 2$ can be expected in the range of $r_{m=2}/a = 0.54 \div 0.68$, which yields the poloidal velocity of magnetic island

$$v_r = \omega r_{m=2} = 6.5 \div 7.8 \ km/s \quad . \tag{4}$$

This value seems to be reasonable since such velocities have been measured on another tokamaks as well (see [4]).

The correlation analysis was applied on shot #3020 for the frequency band related to the m=2 magnetic island (35-60 kHz) and for the broadband part of the spectrum (10-35 kHz) individually to identify dimensions and eventual propagation of the $B_r$ structures in the radial direction. The 2D plots of cross-correlation functions in these two cases are compared in the next figure:

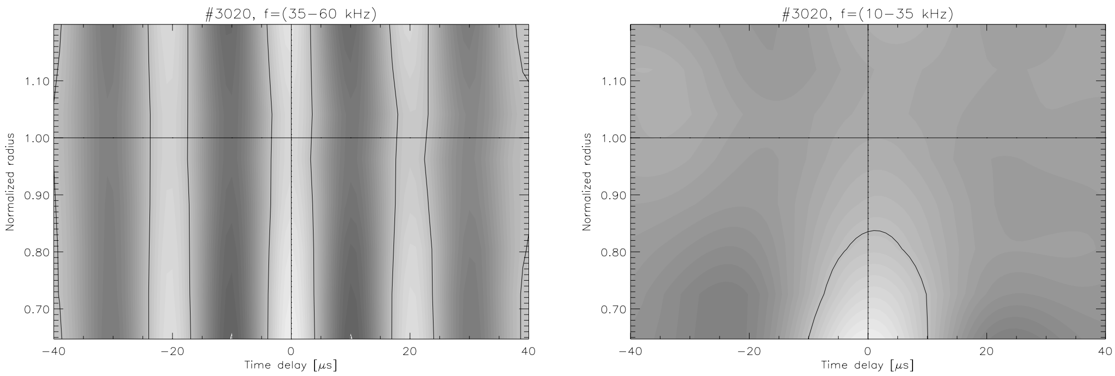


Figure 7: *2D plots of the cross-correlation functions of signals from the 8-coils array for the frequency band f=(35-60 kHz) - right and f=(10-35 kHz) - left, #3020 with q(a)=5.4. Brightness of shading is proportional to the level of cross-correlation. The e-folding drop of the cross-correlation function is emphasized by the solid lines.*

It is seen that for the peak relevant frequencies (35-60 kHz) (left) the probe signals are highly correlated over the whole probe array. The characteristic length of these coherent structures is longer or comparable with the minor radius. For comparison, the right figure shows the cross-correlation functions for the same shot but for the frequency band bellow the spectral peak (10-35 kHz). In this case the correlation is also relatively high, but spatially localized. The corresponding correlation length in the radial direction is $\sim$ 2 cm. Moreover, the radial propagation of broadband microturbulence in outward direction is observed with velocity of about $\sim$ 5 km/s. On the other hand, no such phenomenon is seen for the 'peak' frequencies.

Finally, the frequency resolved radial profiles of $\tilde{B}_r$-fluctuations were computed. The root means square values of signals are computed in the frequency domain individually for the broadband fluctuations and for the coherent mode.

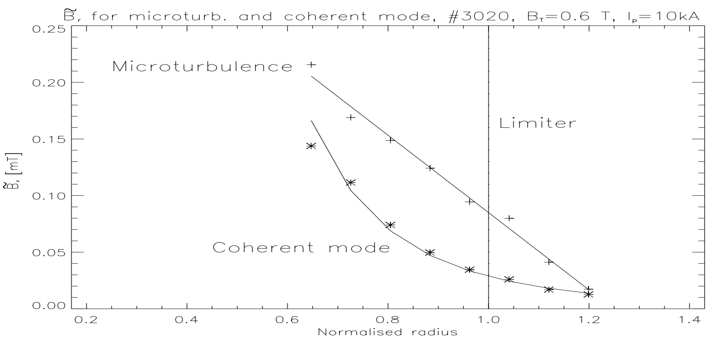


Figure 8: *Radial profiles of microturbulence (broadband part of the signal) and the m=2 magnetic island (signal related to the spectral peak) for shot with q(a)=5.4 (#3020, $I_p$=10 kA, $B_T$=0.6 T).*

The amplitudes of both the components are comparable at all the radial positions, while the form of their radial profiles differ significantly. The profile of microturbulence is well approximated by linear dependence, the coherent mode decays toward the plasma edge as $\sim r^{-4}$.

### 3. Conclusions

The level of magnetic turbulence is monitored and characterized with radial and poloidal resolution on the CASTOR tokamak. Measured level of $\tilde{B_r}$ fluctuations $0.3 \div 0.04\ mT$ is sufficient to account for particle and energy transport in CASTOR. According to the Rechester-Rosenbluth formula, these values of $\tilde{B_r}$ imply the diffusion coefficient $\sim 1\ m^2/s$, which is typical for tokamak plasmas. Magnetic turbulence is composed from two components, the broadband fluctuations caused by microinstabilities and the coherent mode. The presence of the coherent mode is associated with the rotation of m=2 magnetic island within the plasma column.

### References


[1] D.E. Graessle, S.C. Prager, R.N. Dexter: Q dependence of magnetic turbulence in a tokamak, Phys. Fluids B3(9), 1991

[2] I. Ďuran: Fluctuations of magnetic field in the CASTOR tokamak, diploma work, Faculty of Nuclear Sciences and Physical Engineering, Czech Technical University, 1997

[3] J. Stöckel, et all: Analysis of electrostatic and magnetic fluctuations on the CASTOR tokamak, Proceedings of International Conference on Plasma Physics, Nagoya, september 1996, Vol. 1, pages 322-325

[4] G. Vayakis : Anomalous transport in the tokamak edge, PhD thesis, Department of Engineering Science, University of Oxford, 1991



### Acknowledgements

This work is performed in the frame of grant G-IA A1043701 (Grant Agency of Czech Academy of Sciences) and supported by the IAEA contract 6702/R3. Authors are indebted to R. Klíma and L. Krlín for valuable discussions.